Mon. Not. R. Astron. Soc. **000**, 000–000 (0000) Printed 2 February 2008 (MN LATEX style file v2.2)

Nonlinear pulsations in differentially rotating neutron stars: Mass-shedding-induced damping and splitting of the fundamental mode

Nikolaos Stergioulas[(1)], Theocharis A. Apostolatos[(2)], and José A. Font[(3)]
(1)*Department of Physics, Aristotle University of Thessaloniki, Thessaloniki 54124, Greece*
(2)*Department of Physics, National and Kapodistrian University of Athens, Panepistimiopolis, Athens 15783, Greece*
(3)*Departamento de Astronomía y Astrofísica, Universidad de Valencia, Dr. Moliner 50, 46100 Burjassot (Valencia), Spain*

2 February 2008

ABSTRACT
We study small-amplitude, nonlinear pulsations of uniformly and differentially rotating neutron stars employing a two-dimensional evolution code for general-relativistic hydrodynamics. Using Fourier transforms at several points inside the star, both the eigenfrequencies and two-dimensional eigenfunctions of pulsations are extracted. The centrifugal forces and the degree of differential rotation have significant effects on the mode-eigenfunction. We find that near the mass-shedding limit, the pulsations are damped due to shocks forming at the surface of the star. This new damping mechanism may set a small saturation amplitude for modes that are unstable to the emission of gravitational waves. After correcting for the assumption of the Cowling approximation (used in our numerical code), we construct empirical relations that predict the range of gravitational-wave frequencies from quasi-periodic post-bounce oscillations in the core collapse of massive stars. We also find that the fundamental quasi-radial mode is split, at least in the Cowling approximation and mainly in differentially rotating stars, into two different sequences.

1 INTRODUCTION

When neutron stars are formed as a result of a violent event (a core collapse, an accretion-induced collapse, or a binary neutron star merger), they are expected to pulsate nonlinearly before various dissipative effects, such as viscosity, magnetic braking and shock formation, settle them down to a near-equilibrium configuration. All these violent events could lead to high rotational rates for the final objects, due to angular momentum conservation. Moreover, the final object is expected to rotate differentially, since the initial distribution of angular momentum has to be redistributed after collapse or merger. Several axisymmetric and nonaxisymmetric pulsation modes are expected to be excited during neutron star formation and could be important sources of gravitational waves. In addition, some modes could become unstable to the emission of gravitational radiation. The successful detection and identification of pulsation modes requires a detailed understanding of the eigenfrequency and eigenfunction of each mode-sequence, especially since pulsation modes are high-frequency gravitational-wave sources. In addition, it is necessary to have a good understanding of the various damping mechanisms that will operate.

There are several fundamental questions that have to be resolved before we can realistically hope for detection of gravitational waves from neutron star pulsations: *Can neutron stars attain high angular momentum at birth? How strongly differential is the initial rotational profile? What kind of modes are excited? What is the initial amplitude for each mode? What is the frequency for each mode? Which mechanisms dampen the pulsations and on what timescale?* To date, none of the above questions has a definitive answer, but some partial understanding is emerging.

Initial rotation rate: Naively, the collapse of a rotating stellar core should lead to an extremely rapidly rotating neutron star, just by the argument of angular momentum conservation. This picture is, however, made more complicated due to the presence of magnetic fields, wind-mass loss, centrifugal hangup during collapse, fall-back accretion and pre- or post-collapse binary interactions. In recent work by Heger et al. (2003) who consider evolutionary sequences of realistic rotating pre-collapse cores, it is suggested that the initial rotational period of a neutron star can indeed be of the order of 1ms or less, if the magnetic field is neglected. However, if the star passes through a red-supergiant phase, then the dynamo model for magnetic braking of the angular velocity (Spruit, 2002), increases the initial period of proto-neutron stars to several milliseconds. Wind-mass loss during a Wolf-Rayet/helium-star phase (Heger & Woosley, 2003) is another mechanism for slowing down the core of an evolved star. Nevertheless, more rapidly rotating proto-neutron stars could be obtained through other formation scenarios, such as fall-back accretion (see Watts & Andersson, 2002, and references therein), pre-supernova binary interactions (Pfahl et al. 2002; Ivanova & Podsiadlowski, 2003; Podsiadlowski et al. 2003) and post-supernova accretion from a binary com-

panion (Langer et al. 2003). A new scenario for millisecond-pulsar birth in globular clusters is the merger of binary white dwarfs (Middleditch, 2003).

Recently, Villain et al. (2003) have studied in detail the quasi-stationary evolution from core collapse to the formation of a neutron star and find that in most cases an initially hot proto-neutron star contracts and spins-up on a time-scale of seconds, until reaching high rotation rates with $T/|W| > 0.1 - 0.2$, (where T is the kinetic energy and W is the gravitational binding energy of the star). If the initial core is rapidly rotating, centrifugal hangup can occur during collapse. The rotational evolution of a proto-neutron star can also be affected by the details of the high-density equation of state (EOS hereafter), e.g., the appearance of hyperons in the core can yield a very rapidly rotating, but metastable, compact star (Yuan & Heyl, 2003). Axisymmetric core collapse simulations in general relativity (Dimmelmeier, Font & Müller, 2001, 2002a, 2002b; Shibata, 2003) and in Newtonian gravity but with realistic initial conditions (Ott et al. 2003; Kotake, Tamada & Sato, 2003; see also Fryer et al. 2002 and references therein) have also shown the formation of rapidly rotating neutron stars.

Differential rotation: The core collapse studies by Dimmelmeier et al. (2001, 2002a, 2002b), and a quasi-equilibrium treatment by Liu & Lindblom (2000) in the case of accretion-induced collapse of white dwarfs, have shown that rapidly rotating proto-neutron stars are born with a modest degree of differential rotation. A recent detailed analysis by Villain et al. (2003) shows that the length-scale on which the angular velocity changes within the star is of the order of 7-10 km. Hypermassive neutron stars created in a binary merger also have moderate differential rotation, with a somewhat shorter length-scale than in core collapse (see e.g., Shibata & Uryū, 2000). A fundamental question about the rotational profile is how quickly it will become uniform. Shapiro (2000) and Cook, Shapiro & Stephens (2003) have suggested that magnetic braking could drive the star to uniform rotation on a timescale of only seconds. A more recent study by Liu & Shapiro (2003) shows that a magnetic field will cause turbulent motions in a differentially rotating star, driving it to uniform rotation. It has also been suggested that a differentially rotating, viscous proto-neutron star will be brought to uniform rotation due to turbulent mixing on a much shorter timescale (Hegyi, 1977), however, more detailed computations, including realistic composition gradients, are required in order to obtain better estimates.

Mode excitation: In the rotational core collapse simulations by Dimmelmeier et al. (2001, 2002a, 2002b) the proto-neutron star quickly settles into quasi-equilibrium after core bounce. Still, pulsations are excited and survive for several oscillation periods. The dominant pulsation modes that are expected to be excited in rotational core collapse are the quasi-radial ($l = m = 0$) mode and the quadrupole ($l = 2, m = 0$) mode. Due to rotational couplings of non-radial terms in its eigenfunction, the quasi-radial mode becomes a strong emitter of gravitational waves in rapidly rotating stars (it could, in fact, become the dominant mode in which gravitational waves are emitted). The amplitude of the oscillations in the density is estimated as several percent at the center of the star. Newtonian simulations (e.g., Mönchmeyer et al. 1991; Zwerger & Müller, 1997) also reached similar conclusions (for a recent review of core collapse simulations see New, 2002). In the simulations of binary neutron star mergers by Shibata and Uryū (2000, 2002), quasi-periodic oscillations are excited, through which strong gravitational waves are emitted. The frequency of these oscillations suggest that they could correspond to specific non-axisymmetric normal modes of the star. In addition to the non-axisymmetric modes, the axisymmetric quasi-radial mode could also be excited.

Unstable Modes: In both proto-neutron stars and hypermassive neutron stars created in binary mergers, gravitational radiation can drive several modes unstable, through the CFS mechanism (for a review, see e.g. Friedman & Lockitch, 2001), provided the star is rotating sufficiently rapidly. In relativistic stars, the $l = m = 2$ f-mode becomes unstable when $T/|W| > 0.07$ for uniform rotation (Stergioulas & Friedman, 1998; Morsink, Stergioulas & Blattnig, 1999) and at somewhat larger $T/|W|$ for differentially rotating stars (Yoshida et al. 2002). The $l = m = 2$ r-mode can become unstable at considerably lower rotation rates (for a review see Kokkotas & Andersson, 2001). The suppression of the r-mode instability by the presence of hyperons in the core (Jones, 2001; Linblom & Owen, 2002) is not expected to operate efficiently in rapidly rotating stars, since the central density is probably too low to allow for hyperon formation. Moreover, van Dalen & Dieperink (2003) find the contribution of hyperons to the bulk viscosity to be two orders of magnitude smaller than previously estimated. If accreting neutron stars in Low Mass X-Ray Binaries (LMXB, considered to be the progenitors of millisecond pulsars) are shown to reach high masses of $\sim 1.8 M_{\odot}$, then the EOS could be too stiff to allow for hyperons in the core (for recent observations that support a high mass for some millisecond pulsars see Nice, Splaver & Stairs, 2003). Both the f-mode and the r-mode, when unstable, will grow on a timescale of several seconds.

Frequency of excited modes: Even though in a typical nonrotating neutron star the fundamental radial and quadrupole modes have frequencies larger than about 1.5 kHz, in the rapidly rotating models created in core collapse simulations, the frequency of these modes is significantly reduced to well below 1 kHz (Dimmelmeier et al. 2002b), which is within the sensitivity window of current gravitational-wave detectors, such as VIRGO, GEO600, TAMA and LIGO. The large reduction in frequency is due to the fact that differential rotation allows much lower central densities than uniform rotation. In the case of a binary merger, the simulations by Shibata & Uryū (2002) have shown quasi-periodic oscillations of a few kHz. The r-mode, if unstable, would emit gravitational waves at a high frequency of 4/3 the rotational frequency. These sources of gravitational waves are very interesting for the proposed wide-band dual sphere detector (Cerdonio et al. 2001). When the f-mode becomes unstable, it can have an initial frequency of several hundred Hz, which then reduces to zero as the star spins down and approaches the rotation rate at which the mode becomes stable again. Therefore, the f-mode would ideally sweep through the sensitivity window of current laser-interferometric detectors, provided it can grow to a sufficiently large nonlinear amplitude (Lai & Shapiro, 1995).

Damping of pulsations: The stable pulsations excited in the relativistic and Newtonian rotational core collapse simulations are seen to be strongly damped. In an isolated star,

quasi-radial modes are thought to be damped mainly by shear viscosity and gravitational radiation (on a timescale of at least thousands of oscillation periods). In principle, any pulsation of a magnetized star will also be damped by the magnetic field (see e.g. McDermott et al. 1984; Carroll et al. 1986). In the case of quasi-radial pulsations of proto-neutron stars, however, we do not have specific estimates for the corresponding damping time. Once excited, the quasi-radial mode would be an ideal long-term monochromatic source of gravitational waves. However, the strong damping seen in the above simulations reveals that a different mechanism operates in a proto-neutron star, immediately after core bounce (Pons 2003). The strong damping is due to the presence of a high-entropy envelope, which surrounds the newly created neutron star immediately after its birth. The quasi-radial oscillations penetrate into the envelope and are not properly reflected by a sharp surface (as happens in the case of an isolated star). The envelope thus absorbs much of the initial pulsation energy on a dynamical timescale (a similar damping has been observed in nonlinear evolutions of unstable relativistic stars, forced to migrate to the stable branch of equilibrium models, see Font et al. 2002). By the time the proto-neutron star cools down (on a timescale of several seconds) the initial pulsation amplitude has diminished. Therefore, the expected gravitational-wave signal from pulsations in core collapse will be strongly damped.

In order to model the expected signal, a detailed analysis of the damping mechanism is required (taking into account various factors, such as the EOS, the initial rotating stellar core etc.). The unstable f- and r-modes grow on a timescale of the order of several seconds or longer, by which time the initial pulsations have been dramatically damped. In the case of a binary merger, a high-entropy envelope will also form. Its extent will depend on the mass ratio of the two stars – an equal-mass irrotational binary could create only a small envelope, which will not dampen the pulsations as quickly as in a core collapse, while an unequal-mass binary merger could result in a somewhat larger envelope being formed (see Shibata, Taniguchi & Uryū, 2003) and consequently in a stronger damping of quasi-periodic pulsations. In any case, the quasi-periodic oscillations in a binary merger will be much more long-lived than in a core collapse.

Pulsation modes of rapidly rotating stars, assuming uniform rotation, have been computed by Yoshida and Eriguchi (1999, 2001), Font, Stergioulas & Kokkotas (2000), Font et al. (2001) and Stergioulas & Font (2001) in the Cowling approximation (in which spacetime perturbations are neglected). In full general relativity, Stergioulas & Friedman (1998) and Morsink, Stergioulas & Blattnig (1999) computed the onset of the $l = m = 2$ f-mode instability, while Font et al. (2002) computed the frequencies of the two lowest-order quasi-radial modes. For differentially rotating stars, the only existing computation is by Yoshida et al. (2002), who obtained the $l = m = 2$ f-mode frequencies for a moderate strength of differential rotation. Nonlinear effects of radial pulsations in nonrotating relativistic stars have been studied by Sperhake, Papadopoulos & Andersson (2001) (see also Sperhake, 2002).

In the present paper, we study in detail two different sequences of uniformly and differentially rotating relativistic polytropes, and obtain the eigenfrequencies and eigenfunctions of several pulsations modes in the Cowling approximation. For a sequence of fixed central energy density the mode-frequencies are only weakly affected by the rotation rate. However, for a sequence of fixed rest mass, the mode frequencies continuously decrease as the rotation rate increases (and the central density decreases). An interesting result of our study is that the fundamental quasi-radial mode splits into two different modes, an effect which is more prominently seen in differentially rotating models. Based on the frequency spectrum of nonrotating and uniformly rotating stars, this split is not expected. If it turns out not to be really a new mode, it could be due to the fact that in the Cowling approximation the energy and momentum conservation are violated. For example, this violation leads to the appearance of an unphysical "fundamental" dipole mode in simulations of nonrotating stars (Font et al. 2001). Another important outcome of our investigation is that when studying the excitation of quasi-radial pulsations in rapidly rotating models (which are near their mass-shedding limit) we find that the pulsations are damped because of mass-shedding in the equatorial region. This new damping mechanism could set a severe limit on the saturation amplitude of unstable modes.

The rest of the paper is organized as follows. In Section 2 we outline our computational method, while in Section 3 we describe the equilibrium properties of all initial models we subsequently evolve. In Section 4 the eigenfrequencies and eigenfunctions of pulsating stars are presented while Section 5 focuses on the splitting of the fundamental mode. Sections 6 and 7 discuss the damping of pulsations due to mass-shedding and the implications of our results on the detection of gravitational waves, respectively. Finally, a summary and a discussion of our results is presented in Section 8.

2 OUTLINE OF COMPUTATIONAL METHOD

We study the axisymmetric pulsations of rapidly rotating relativistic stars by first constructing several sequences of uniformly and differentially rotating equilibrium models, as described in detail in Section 3. The equilibrium models assume a relativistic polytropic EOS of the form

$$p = K\rho^{1+1/N}, \quad (1)$$

$$\varepsilon = \rho + Np, \quad (2)$$

where p is pressure, ε is energy density, ρ is rest-mass density, N is the polytropic index and K is the polytropic constant. Unless otherwise noted, we choose dimensionless units for all physical quantities by setting $c = G = M_\odot = 1$.

The nonlinear time-evolutions of perturbed equilibrium models are carried out using the same numerical hydrodynamics code developed by Font et al. (2001, 2002). Suitable perturbations of selected equilibrium variables are added to the equilibrium model, in order to excite specific modes. In the absence of the true eigenfunction of a given mode, each perturbation is chosen so as to mimic the angular dependence of the eigenfunction of the corresponding mode of a slowly-rotating Newtonian star. Usually, this ensures that the chosen mode will dominate the time-evolution at least for the slower rotating models. However, since the perturbation is not exact, additional pulsation modes will be excited,

especially for rapidly rotating models. For the $l = 0$ modes a density perturbation is used, of the form

$$\delta\rho = a\rho_c \sin\left(\pi \frac{r}{r_s(\theta)}\right), \tag{3}$$

where ρ_c is the central density of the star and $r_s(\theta)$ is the coordinate radius of the surface of the star. The constant a is the amplitude of the perturbation, which we normally take to be of the order of 1%. The $l = 2$ modes are excited, by perturbing the θ-component of the four-velocity as follows:

$$u_\theta = a \sin\left(\pi \frac{r}{r_s(\theta)}\right) \sin\theta\cos\theta, \tag{4}$$

(see Font et al. 2001 for more details).

The perturbed models are evolved in time with a two-dimensional general-relativistic hydrodynamics code, in which we have implemented a Godunov-type scheme based on the Marquina flux formula and the 3rd-order PPM reconstruction (see Font et al. 2000, 2001; see also Font, 2003, for a review of Godunov-type schemes in general relativistic hydrodynamics). Keeping the spacetime fixed to the initial equilibrium state during the evolution corresponds to the Cowling approximation in perturbation theory. Below the mass-shedding limit (see Friedman, Ipser & Parker, 1986, for the precise definition of the mass-shedding limit in the case of rapidly rotating relativistic stars), we assume that the star remains isentropic by enforcing the EOS (1),(2). Near the mass-shedding limit, when shocks form (see Section 6), the adiabatic ideal fluid EOS is used instead

$$p = (\Gamma - 1)\rho\epsilon, \tag{5}$$

where $\Gamma = 1 + 1/N$ and ϵ is the specific internal energy. Notice that at the initial time the isentropic equilibrium models constructed with the polytropic EOS (1),(2) are consistent with the ideal fluid EOS (5).

The time series of the evolved perturbations are Fourier analyzed, and the peaks in the corresponding spectra are identified with specific pulsation modes, starting from the nonrotating member of the sequence, where the pulsation frequencies are known from perturbation theory. As the rotation rate increases, it becomes increasingly more difficult to identify specific modes in the Fourier spectrum. For this reason, we also extract the eigenfunction for each peak in the Fourier spectrum and use it as an additional criterion to identify specific modes (see Section 4).

3 EQUILIBRIUM MODELS

Equilibrium models of rotating relativistic stars are constructed using the numerical code `rns` (Stergioulas & Friedman, 1995) which was extended to include differential rotation. Extensive tests of the accuracy of the code in the case of uniform rotation can be found in Nozawa et al. (1998) and in Stergioulas (2003). The metric describing an axisymmetric relativistic star is assumed to have the usual form

$$ds^2 = -e^{\gamma+\rho}dt^2 + e^{\gamma-\rho}r^2\sin^2\theta(d\phi - \omega dt)^2 + e^{2\alpha}(dr^2 + r^2 d\theta^2), \tag{6}$$

where the metric functions γ, ρ, ω and α depend on the coordinates r and θ only[1]. Axisymmetry enforces the specific angular momentum measured by the proper time of matter $j \equiv u^t u_\phi$ to be a function of the angular velocity Ω only. A different specific angular momentum

$$\tilde{j} = u_\phi \left(\frac{\varepsilon + p}{\rho}\right), \tag{7}$$

is locally conserved during the phase of homologous collapse of a rotating star. The Rayleigh criterion for local dynamical stability to axisymmetric perturbations is

$$\frac{d\tilde{j}}{d\Omega} < 0. \tag{8}$$

The simplest common choice of the differential rotation law $j = j(\Omega)$ that satisfies the Rayleigh stability criterion (see Komatsu, Eriguchi & Hachisu, 1989a,b) leads to an angular velocity distribution of the form

$$\Omega_c - \Omega = \frac{1}{A^2}\left[\frac{(\Omega-\omega)r^2\sin^2\theta e^{-2\rho}}{1-(\Omega-\omega)^2 r^2\sin^2\theta e^{-2\rho}}\right], \tag{9}$$

where Ω_c is the angular velocity on the rotational axis and A is a parameter with units of length, that determines the length scale over which the angular velocity varies inside the star (in the limit of $A \to \infty$, uniform rotation is recovered).

When constructing sequences of fixed rest mass, the radius of the star can vary by more than a factor of two. If one would characterize the sequence by a fixed value of the parameter A, then different models would correspond to different degrees of differential rotation. In order to ascribe the same degree of differential rotation to all models along a sequence, we follow Baumgarte, Shapiro & Shibata (2000) in normalizing the parameter A by the radius of the star. Thus, we define

$$\hat{A} = A/r_e, \tag{10}$$

where $\hat{A}$ is now a dimensionless parameter and r_e is the equatorial coordinate radius of the star. Notice that in the Newtonian limit, $\hat{A}$ is the radius of the cylinder, as a fraction of the radius of the star, where the angular velocity falls to one half of the central angular velocity.

Our focus is on the effect of rotation on pulsation modes. Hence, we do not survey a broad range of suggested high-density equations of state, but rather choose a polytropic EOS with $N = 1$ and $K = 100$, respectively. This choice corresponds to models of neutron stars having mass and radius similar to those constructed with a realistic EOS of average stiffness. We focus attention on two different sequences of differentially rotating models (sequences A and B) and their uniformly rotating counterparts (sequences AU and BU). The equilibrium properties of all models are displayed in Table 1. All sequences terminate at the same nonrotating model (thus, models A0, AU0, B0 and BU0 all coincide).

The differentially rotating sequence A and its corresponding uniformly rotating sequence AU are characterized by a fixed rest mass $M_0 = 1.506 M_\odot$. Along sequence A, the degree of differential rotation is held fixed at $\hat{A} = 1$.

[1] The metric function ρ in Eq. (6) should not be confused with the rest-mass density in Eq. (1).

Table 1. Properties of the four sequences of equilibrium models (A is a sequence of fixed rest mass $M_0 = 1.506 M_\odot$ with $\hat{A} = 1$, AU is the corresponding sequence of uniformly rotating models, B is a sequence of fixed central rest mass density $\rho_c = 1.28 \times 10^{-3}$ with $\hat{A} = 1$, and BU is the corresponding sequence of uniformly rotating models). All models are relativistic polytropes with $N = 1$ and $K = 100$. The definitions of the various quantities are given in the main text. Notice that all quantities are in dimensionless units with $c = G = M_\odot = 1$.

model	ε_c ($\times 10^{-3}$)	M	R	r_e	r_p/r_e	Ω_c ($\times 10^{-2}$)	Ω_e ($\times 10^{-2}$)	$T/\|W\|$
A0	1.444	1.400	9.59	8.13	1.0	0.0	0.0	0.0
A1	1.300	1.405	10.01	8.54	0.930	0.202	0.076	0.018
A2	1.187	1.408	10.40	8.92	0.875	0.258	0.098	0.033
A3	1.074	1.410	10.84	9.35	0.820	0.294	0.113	0.049
A4	0.961	1.413	11.37	9.87	0.762	0.319	0.123	0.066
A5	0.848	1.418	12.01	10.49	0.703	0.334	0.130	0.086
A6	0.735	1.422	12.78	11.25	0.643	0.338	0.134	0.107
A7	0.622	1.427	13.75	12.21	0.579	0.334	0.134	0.131
A8	0.509	1.433	15.01	13.45	0.513	0.320	0.130	0.158
A9	0.396	1.439	16.70	15.13	0.444	0.295	0.122	0.189
A10	0.283	1.447	19.03	17.44	0.370	0.260	0.110	0.223
A11	0.170	1.456	21.92	20.30	0.294	0.218	0.094	0.260
AU0	1.444	1.400	9.59	8.13	1.0	0.0	0.0	0.0
AU1	1.300	1.404	10.19	8.71	0.919	1.293	1.293	0.020
AU2	1.187	1.407	10.79	9.30	0.852	1.656	1.656	0.037
AU3	1.074	1.411	11.56	10.06	0.780	1.888	1.888	0.055
AU4	0.961	1.415	12.65	11.14	0.698	2.029	2.029	0.076
AU5	0.863	1.420	14.94	13.43	0.575	2.084	2.084	0.095
B0	1.444	1.400	9.59	8.13	1.0	0.0	0.0	0.0
B1	1.444	1.437	9.75	8.24	0.950	0.180	0.067	0.013
B2	1.444	1.478	9.92	8.36	0.900	0.257	0.094	0.026
B3	1.444	1.525	10.11	8.49	0.849	0.319	0.116	0.040
B4	1.444	1.578	10.31	8.63	0.800	0.373	0.134	0.055
B5	1.444	1.640	10.53	8.77	0.750	0.423	0.150	0.071
B6	1.444	1.713	10.76	8.91	0.700	0.471	0.165	0.087
B7	1.444	1.798	11.01	9.05	0.650	0.519	0.179	0.105
B8	1.444	1.899	11.26	9.17	0.600	0.568	0.192	0.124
B9	1.444	2.020	11.50	9.26	0.550	0.623	0.205	0.144
B10	1.444	2.167	11.71	9.27	0.500	0.689	0.219	0.165
B11	1.444	2.341	11.80	9.13	0.450	0.777	0.236	0.187
B12	1.444	2.532	11.64	8.72	0.400	0.912	0.258	0.207
BU0	1.444	1.400	9.59	8.13	1.00	0.0	0.0	0.0
BU1	1.444	1.432	9.83	8.33	0.95	1.075	1.075	0.012
BU2	1.444	1.466	10.11	8.58	0.90	1.509	1.509	0.024
BU3	1.444	1.503	10.42	8.82	0.85	1.829	1.829	0.037
BU4	1.444	1.543	10.78	9.13	0.80	2.084	2.084	0.050
BU5	1.444	1.585	11.20	9.50	0.75	2.290	2.290	0.062
BU6	1.444	1.627	11.69	9.95	0.70	2.452	2.452	0.074
BU7	1.444	1.666	12.30	10.51	0.65	2.569	2.569	0.084
BU8	1.444	1.692	13.07	11.26	0.60	2.633	2.633	0.091
BU9	1.444	1.695	13.44	11.63	0.58	2.642	2.642	0.092

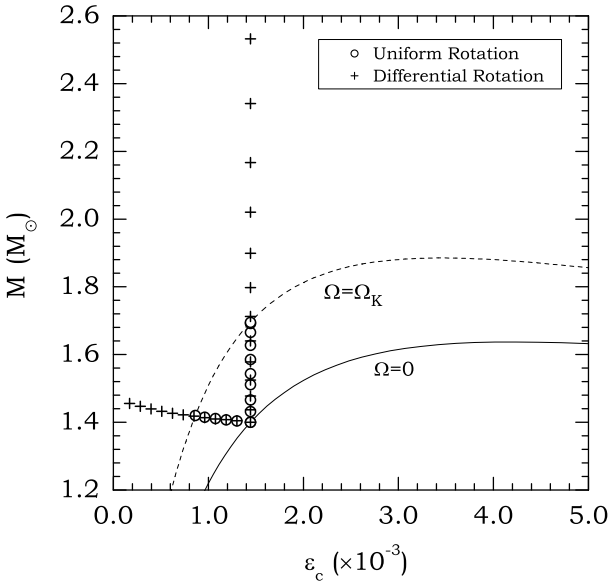

Figure 1. Mass vs. central energy density plot of all models in sequences A, AU, B and BU. Open circles correspond to uniformly rotating models, while the crosses correspond to differentially rotating models. The two nearly horizontal sequences are A and AU, while the two vertical sequences are B and BU. Also shown are the sequence of nonrotating models (solid line), and the sequence of models rotating at the mass-shedding limit for uniform rotation (dashed line). Differential rotation allows equilibrium models well beyond the region allowed for uniformly rotating models.

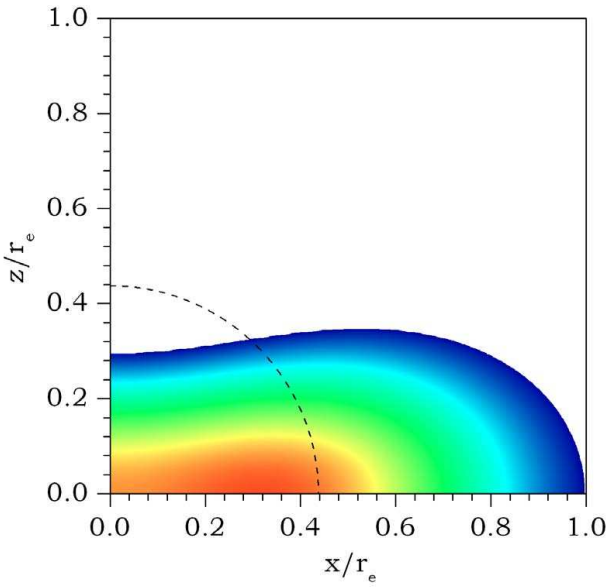

Figure 2. Density stratification in the fastest differentially rotating model of the fixed rest-mass sequence A. The maximum density appears off-center, at $x/r_e = 0.32$. In comparison, the shape of the nonrotating star of same rest mass is shown (dashed line), scaled by the equatorial radius of the rotating model.

The values of M_0 and $\hat{A}$ are chosen in order to represent a newly-born, differentially rotating neutron star. The angular velocity at the equator is roughly 1/3 to 1/2 of the central angular velocity, which is similar to the degree of differential rotation obtained in typical core collapse simulations (see Villain et al. 2003). The fastest rotating model in sequence A has a polar to equatorial coordinate axes ratio of only $r_p/r_e = 0.294$, a ratio $T/|W| = 0.26$ and rotates close to, but still below, the mass-shedding limit. The central density is nearly an order of magnitude smaller than the corresponding nonrotating model, while the circumferential radius is more than twice as large. The uniformly rotating sequence AU only reaches an axes ratio of 0.575, a ratio $T/|W| = 0.095$, half the central density, and a 50% larger radius than the corresponding nonrotating model. Model AU5 is at the mass-shedding limit.

On the other hand, the differentially rotating sequence B and its corresponding uniformly rotating sequence BU are characterized by a fixed central density $\rho_c = 1.28 \times 10^{-3}$ and fixed $\hat{A} = 1$. Its fastest rotating member has rest mass of $M_0 = 2.79 M_\odot$ and a gravitational mass of $2.53 M_\odot$, corresponding roughly to a hypermassive neutron star created in a binary neutron star merger. The degree of differential rotation is in rough agreement with simulations by Shibata & Uryū (2000, 2002). The axes ratio for the fastest rotating model is 0.4 (the model being still below, but close to, the mass-shedding limit). Since all models in the sequence are compact, the radius R only increases by 21%. The corresponding uniformly rotating sequence only reaches an axes ratio of 0.58 at the mass-shedding limit (BU9) with an increase in radius R by 40%. Thus, we see that when considering a sequence of fixed central density, the uniformly rotating models attain a larger equatorial radius than differentially rotating models, which tend to expand out of the equatorial plane, becoming torus-like.

Fig. 1 shows all constructed equilibrium models in a mass vs. central energy density plot. The two nearly horizontal sequences are A and AU, while the two vertical sequences are B and BU. Open circles correspond to uniformly rotating models, while the crosses correspond to differentially rotating models. Also shown are the sequence of nonrotating models (solid line) and the sequence of models rotating at the mass-shedding limit for uniform rotation (dashed line). Differential rotation allows equilibrium models well beyond the region allowed for uniformly rotating models (see also Baumgarte, Shapiro & Shibata, 2000, where such configurations are called *hypermassive*).

In Fig. 2 the density stratification for the fastest rotating model of sequence A (A11) is shown. In the figure, Cartesian coordinates, $x = r \sin\theta, z = r \cos\theta$ are used, scaled by the equatorial coordinate radius r_e. The maximum density is attained off-center. The dashed line shows the spherical surface of the nonrotating model with the same rest mass (A0), scaled by the equatorial coordinate radius of the rotating model A11. It becomes evident that the large rotation rate of model A11 causes the equatorial radius to increase by more than a factor of two.

Finally, we note that apart from the above two sequences, we have also investigated the effect of the degree of differential rotation on the axisymmetric pulsations, by constructing various sequences that differ only in the value of $\hat{A}$.

Table 2. Frequencies of the fundamental quasi-radial ($l = 0$) mode, F, its first overtone, H_1, the fundamental quadrupole ($l = 2$) mode, ${}^2f$ and its first overtone, ${}^2p_1$, for the sequence of uniformly rotating models AU.

model	F kHz	H_1 kHz	${}^2f$ kHz	${}^2p_1$ kHz
AU0	2.706	4.547	1.846	4.100
AU1	2.526	4.246	1.800	3.862
AU2	2.403	4.090	1.744	3.592
AU3	2.277	3.937	1.663	3.265
AU4	2.141	3.795	1.547	2.847
AU5	1.960	3.647	1.330	2.560

Table 3. Same as Table 2, but for the sequence of differentially rotating models A. Also shown are the frequencies of an additional fundamental mode $F_{\rm II}$ that appears mainly in differentially rotating models (at least in the Cowling approximation).

model	$F_{\rm II}$ kHz	F kHz	H_1 kHz	${}^2f$ kHz	${}^2p_1$ kHz
A0	2.706	2.706	4.547	1.846	4.100
A1	2.485	2.561	4.310	1.822	3.961
A2	2.361	2.480	4.163	1.780	3.822
A3	2.243	2.386	4.029	1.738	3.642
A4	2.142	2.295	3.900	1.677	3.442
A5	2.039	2.201	3.748	1.598	3.211
A6	1.921	2.101	3.563	1.510	2.973
A7	1.779	1.982	3.329	1.403	2.711
A8	1.609	1.846	3.120	1.274	2.494
A9	1.424	1.667	2.857	1.132	2.185
A10	1.223	1.422	2.503	0.966	1.905
A11	1.044	1.220	2.174	0.820	1.658

Table 4. Same as Table 2, but for the sequence of uniformly rotating models BU.

model	F kHz	H_1 kHz	${}^2f$ kHz	${}^2p_1$ kHz
BU0	2.706	4.547	1.846	4.100
BU1	2.657	4.467	1.855	4.040
BU2	2.619	4.409	1.860	3.944
BU3	2.579	4.385	1.857	3.814
BU4	2.535	4.371	1.844	3.645
BU5	2.495	4.356	1.815	3.456
BU6	2.456	4.357	1.762	3.244
BU7	2.417	4.337	1.686	3.010
BU8	2.328	4.300	1.588	2.710
BU9	2.313	4.280	1.558	2.642

Table 5. Same as Table 3, but for the sequence of differentially rotating models B.

model	$F_{\rm II}$ kHz	F kHz	H_1 kHz	${}^2f$ kHz	${}^2p_1$ kHz
B0	2.706	2.706	4.547	1.846	4.100
B1	2.627	2.658	4.446	1.880	4.102
B2	2.561	2.637	4.421	1.900	4.090
B3	2.525	2.632	4.405	1.913	4.045
B4	2.506	2.632	4.403	1.924	3.983
B5	2.487	2.632	4.422	1.929	3.907
B6	2.459	2.633	4.436	1.925	3.828
B7	2.423	2.635	4.447	1.909	3.721
B8	2.394	2.646	4.444	1.890	3.632
B9	2.360	2.653	4.413	1.867	3.567
B10	2.330	2.662	4.360	1.842	3.500
B11	2.318	2.678	4.300	1.832	3.470
B12	2.328	2.722	4.240	1.830	3.473

4 EIGENFREQUENCIES AND EIGENFUNCTIONS

Although we use a nonlinear evolution code to study pulsations of rotating stars, we restrict attention to small-amplitude pulsations (small in the sense that e.g. $\delta\rho/\rho \sim 10^{-2}$). Therefore, the time-evolution of a perturbed star can still be viewed (to a good approximation) as a superposition of linear normal modes. When obtaining the Fourier transform of the time-evolution of several variables, we verify that the various modes that are excited have indeed discrete frequencies (same frequency at any point inside the star in the coordinate frame). Thus, even though the evolution is nonlinear, the amplitude is small enough to justify the use of the terms "eigenfrequency" and "eigenfunction" for the various pulsation modes. In order to compute the real part of the eigenfrequency of a pulsation mode we Fourier-transform the time series of the evolution of a suitable physical variable (the density for the $l = 0$ modes and v_θ for the $l = 2$ modes). Instead of examining the Fourier spectra at a few specific points inside the star, we integrate the amplitude of the Fourier transform along a coordinate line, e.g. for the $l = 0$ modes we examine the integrated Fourier amplitude along $\theta = \pi/2$ (equatorial plane), while for the $l = 2$ modes the integrated Fourier amplitude along a line of $\theta = \pi/4$ is used.

Since the trial-eigenfunction used for exciting the pulsations does not correspond exactly to a particular mode, several additional modes are excited, apart from the main mode one wishes to study. This is particularly true for very rapidly rotating models, where rotational coupling effects are significant and higher-order coupling terms in the mode-eigenfunctions become comparable to the dominant term. Thus, in order to identify specific modes for several models along a sequence, one has to begin with pulsations of a non-rotating star (for which the modes are identified by comparison to results obtained with linear perturbation theory, see Font et al. 2000, 2001, 2002)[2] and gradually identify modes for more rapidly rotating stars by comparing the peaks in a Fourier transform to the corresponding peaks in a more slowly rotating model. Close to the mass-shedding limit, avoided crossings between low-order and high-order modes can complicate the picture and lead to erroneous identifications. For this reason, we do not only rely on the Fourier transforms at a few points inside the star, but reconstruct

[2] For a review of pulsations of nonrotating relativistic stars see Kokkotas & Schmidt (1999).

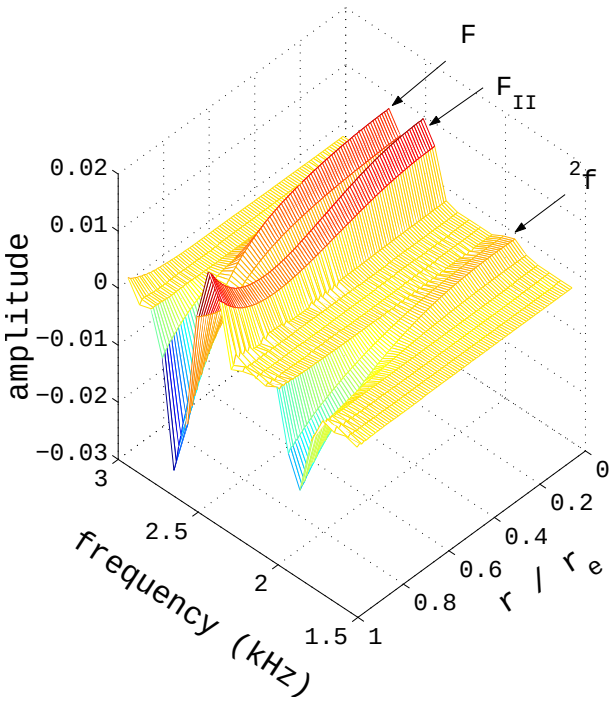

Figure 3. Amplitude of the Fourier transform of the time-evolution of the density in the equatorial plane, for model B7, after applying an $l = 0$ perturbation. Several excited pulsation modes can be identified. For a particular mode, the amplitude of the Fourier transform correlates with its eigenfunction.

the whole two-dimensional eigenfunction of each mode, using Fourier transforms at every point inside the star. At the eigenfrequency of a specific mode, the amplitude of the Fourier transform correlates with its eigenfunction. A change in sign in the eigenfunction corresponds to both the real and imaginary part of the Fourier transform going through zero. Comparing the eigenfunctions corresponding to different peaks in a Fourier transform, allows for an unambiguous identification of specific mode sequences.

A example of the eigenfunction extraction using Fourier transforms is shown in Figure 3, which displays the amplitude of the Fourier transform of the time-evolution of the density, after an $l = 0$ perturbation was applied to model B7. In the range of frequencies shown in Figure 3, the amplitude of the Fourier transform clearly correlates with the eigenfunctions of the fundamental F- and ${}^2f$-modes (the additional mode, $F_{\rm II}$, is discussed in Section 5). Notice that in displaying the eigenfunctions we use the amplitude of the Fourier transform, multiplied by the sign of its real part.

When comparing the eigenfrequencies between models that differ only in the degree of differential rotation, we see that a moderate degree of differential rotation has some (but not dramatic) effect on the eigenfrequencies. When $\hat{A}$ is decreased significantly below ~ 1, which leads to a "strongly" differentially rotating model, most of the angular momentum of the star is concentrated in a narrow region around the rotational axis. Outside this region the star is only slowly rotating and the eigenfrequencies of its pulsations become again similar to those of a nonrotating model. Thus, the effect of differential rotation on the eigenfrequencies becomes strongest, not for very small values of $\hat{A}$ (strong differential rotation), but for values that correspond to stars with only a moderate degree of differential rotation.

4.1 Fixed rest mass sequences

It is well-known that the frequencies of the fundamental $l = 0$ and $l = 2$ polar modes of oscillation depend mainly on the central density of a star, or, equivalently, on the compactness M/R (see e.g. Hartle & Friedman 1975). This is particularly true for the axisymmetric ($m = 0$) modes. The sequences of fixed rest mass $M_0 = 1.506 M_\odot$ start with a nonrotating model with compactness $M/R = 0.15$. Rotation increases the radius and decreases the central density. The uniformly rotating sequence AU terminates at the mass-shedding limit, with a compactness of $M/R = 0.095$. The differentially rotating sequence can reach higher rotation rates and terminates near the mass-shedding limit with a compactness of $M/R = 0.066$. Based on the significant decrease of the compactness along the fixed-rest-mass sequences, we expect a corresponding decrease in the frequencies of the fundamental modes (and a similar tendency for the first overtones).

Table 2 displays the computed eigenfrequencies for the fundamental and first overtone of the $l = 0$ and $l = 2$ modes for the sequence AU. Rotation reduces the frequency of the fundamental quasi-radial mode from 2.71 kHz to 1.96 kHz with corresponding changes in the frequencies of the other modes. Figure 4 displays the variation of the mode-frequencies with increasing $T/|W|$ along sequence AU (dashed lines). The rate of decrease in frequency for the fundamental quasi-radial modes, with increasing rotation rate becomes larger as the mass-shedding limit is approached (due to a cusp forming in the equatorial region), while the decrease in frequency for the other modes is a nearly linear function of $T/|W|$.

Table 3 reports the corresponding eigenfrequencies for the differentially rotating sequence A, which are also shown in Figure 4 (solid lines). The frequencies of all modes decrease nearly linearly with increasing $T/|W|$. Due to the differential rotation, the outer layers of the star rotate slower and the equatorial radius is smaller than a uniformly rotating model of same $T/|W|$. This leads to a smaller sound-crossing time and correspondingly higher fundamental mode frequencies for the differentially rotating models. This explains why the lines in Fig. 4 corresponding to the fundamental modes of sequence A have smaller slopes than those corresponding to sequence AU.

For the fastest rotating model of sequence A, the fundamental quasi-radial mode has a frequency of only 1.22 kHz, with the fundamental quadrupole mode having a frequency of 0.82 kHz. It should be emphasized that the above frequencies are computed in the Cowling approximation, which leads to higher values than the actual frequencies (see Yoshida & Kojima, 1997). Therefore, the actual frequencies of the fundamental quasi-radial modes should be in the range of $40 - 45\%$ smaller than those computed here. The actual frequencies of the fundamental quadrupole mode should be roughly $15 - 20\%$ smaller than our values. For the nonrotating model of sequences A and AU, the actual frequencies of the fundamental $l = 0$ and $l = 2$ modes are 1.44 kHz and 1.58 kHz, respectively (Font et al. 2002). Thus, the fundamental $l = 0$ mode has a frequency only some-

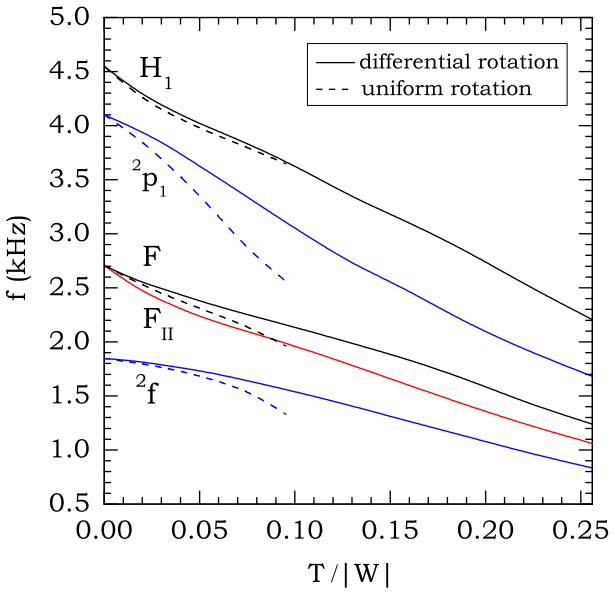

Figure 4. Eigenfrequencies of various modes for sequences A and AU. The lower of the two lines that start at the F-mode frequency for the nonrotating models is an additional mode, $F_{\rm II}$, appearing mainly in differentially rotating stars (at least in the Cowling approximation).

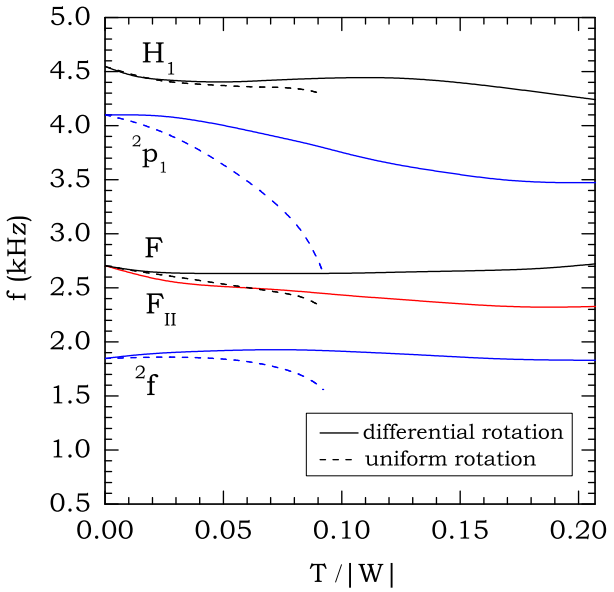

Figure 5. Same as Figure 4, but for the sequences B and BU.

what smaller than the fundamental $l = 2$ mode (while in the Cowling approximation it has a frequency significantly larger than the fundamental $l = 2$ mode).

In Font et al. (2002) it was found that, in the case of uniform rotation, both the actual frequency and the frequency in the Cowling approximation of the fundamental quasi-radial mode decrease in a similar way as the rotation rate increases. This leads to the following empirical relation between the actual frequency and the frequency in the Cowling approximation.

$$f_\Omega = f_\Omega^{(\rm C)} + \left(f_0 - f_0^{(\rm C)}\right), \tag{11}$$

where the superscript (C) denotes the Cowling approximation, f_Ω is the frequency of the fundamental quasi-radial mode for a rotating star with angular velocity Ω, and f_0 is the corresponding frequency in a nonrotating star. This empirical relation was found to be accurate to within 2% at all rotation rates, even near the mass-shedding limit. Since the frequencies of differentially rotating stars are not much different with respect to those of uniformly rotating stars with the same oblateness, the above relation should approximately hold for differentially-rotating models as well.

Based on Yoshida & Kojima (1997) and Yoshida & Eriguchi (2001) we can estimate the error in the fundamental mode frequencies, due to the Cowling approximation. For the fastest rotating model of sequence A, with $M/R \sim 0.07$, we estimate that the actual fundamental $l = 0$ and $l = 2$ frequencies are 63% and 79% of our results in the Cowling approximation, respectively (actual frequency meaning the frequency without the assumption of the Cowling approximation). Taking into account the nearly linear scaling of the frequencies with increasing rotation rate in Figure 4, we construct the following empirical relation

$$f({\rm kHz}) \approx 1.44 - 2.59\frac{T}{|W|}, \tag{12}$$

for the actual frequency of the fundamental quasi-radial mode and

$$f({\rm kHz}) \approx 1.58 - 3.69\frac{T}{|W|}, \tag{13}$$

for the actual frequency of the fundamental quadrupole mode for the differentially rotating models of sequence A. We estimate the uncertainty of the above empirical relations to be on the order of a few percent.

According to the above empirical relations, for rapidly rotating proto-neutron stars with $T/|W|$ in the range $0.14 - 0.26$, the frequency of the two fundamental modes will be in a range of roughly $0.65 - 1.1$ kHz. This range of frequencies agrees well with the frequencies of gravitational waves observed in the rotating core collapse simulations by e.g. Dimmelmeier et al. (2001, 2002a, 2002b), which confirms the validity of our chosen equilibrium models and pulsation modes to model the gravitational waves produced in the above simulations[3].

The additional fundamental frequency $F_{\rm II}$ in Tables 2 and 3 and in Figure 4 is discussed in Section 5.

4.2 Fixed central density sequence

Another sequence of models with differential rotation that has been analyzed is sequence B, consisting of twelve models with the same central energy density $\epsilon_c = 1.28 \times 10^{-3}$ but with axes ratios ranging from 1.0 to 0.40. The most rapidly rotating model corresponds to a hypermassive neutron star, such as those created temporarily in a binary neutron star

[3] Here we only refer to the regular collapse cases in Dimmelmeier et al. and not to multiple-bounce cases. Notice that, even though our polytropic index is different than in Dimmelmeier et al., our choice of the polytropic constant leads to models of similar compactness, for the same mass.

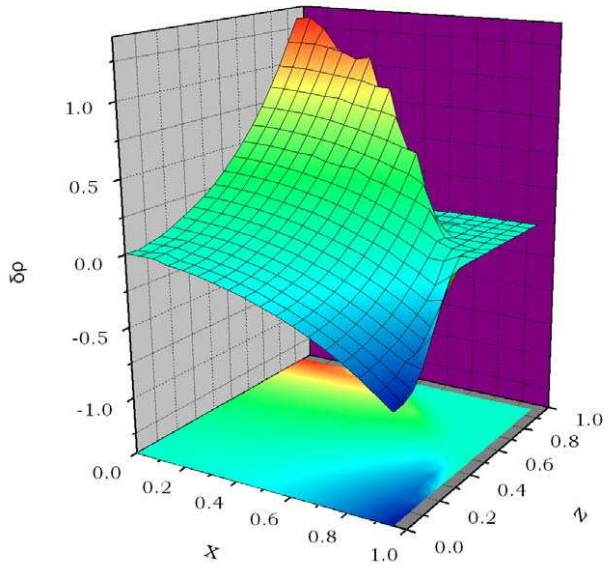

Figure 6. Two-dimensional eigenfunction of the density perturbation, corresponding to the $l = 2$ fundamental mode for the nonrotating model B0. The eigenfunction is shown in Cartesian coordinates with x and z being scaled by the equatorial coordinate radius r_e, while $\delta\rho$ is in arbitrary units.

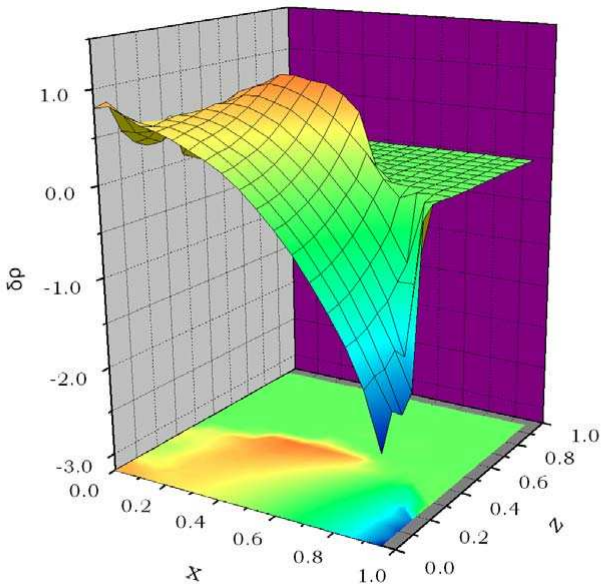

Figure 7. Same as Figure 6, but for the most rapidly rotating model of sequence B (B12).

merger. The corresponding sequence of uniformly rotating models, BU, of same fixed central energy density, comprises models with axes ratios from 1.0 to 0.58. The computed frequencies of the $l = 0, 2$ fundamental modes and their first overtones are shown in Figure 5 and in Tables 4 and 5 (the additional fundamental mode $F_{\rm II}$ is discussed in Section 5).

The frequencies of the fundamental $l = 0$ and $l = 2$ modes changes by as much as 16% along the sequence BU. In comparison, for sequence B the eigenfrequencies for both the $l = 0$ and $l = 2$ fundamental modes remain relatively unaffected by the rotation rate, changing by less than 3% and 5%, respectively, compared to their values in the nonrotating limit. This leads to the conclusion that a moderate amount of differential rotation, of the order of $\hat{A} = 1$, makes the fundamental frequencies relatively insensitive to rotation and depending mainly on the central energy density of the star. This finding should simplify attempts to extract information about the physical properties of neutron stars in binary mergers, when such events become observable through their gravitational-wave emission.

As discussed in Section 2 we obtain the two-dimensional eigenfunction of a specific mode by computing Fourier transforms of selected variables at every point inside the star. An example of such an eigenfunction is shown in Figure 6, which displays the eigenfunction corresponding to the density perturbations due to the $l = 2$ fundamental mode, for the nonrotating model B0. Since the model is nonrotating, the eigenfunction shows the expected quadrupolar structure. For the most rapidly rotating model B12, however, the eigenfunction for the same mode appears severely altered (Figure 7) with respect to the nonrotating limit. There are two main effects caused by rapid rotation. Firstly, the $l = 2$ fundamental mode does not only couple to higher order spherical harmonics, but also to an $l = 0$ term. This causes a significant density variation at the center of the star, whereas for the nonrotating model the center of the star is not pulsating. Secondly, the centrifugal force weakens the effective gravity in the equatorial region, causing the eigenfunction to attain a large amplitude near the equatorial surface of the star. The effect of the centrifugal force becomes extreme when the star rotates at the mass-shedding limit, as discussed in Section 6. The above effects are common in other modes, too, and also in all four sequences considered.

5 SPLITTING OF THE FUNDAMENTAL MODE

An interesting feature visible in Figures 4 and 5 is the appearance of an additional fundamental mode, which we denote as $F_{\rm II}$. This mode is degenerate in the nonrotating limit, but becomes distinct from the F-mode for rotating models. For sequence A, the $F_{\rm II}$-mode has a similar dependence on rotation rate as the F-mode, with the difference in frequency between the two modes remaining nearly constant with increasing rotation rate. For sequence B, however, the frequency of the $F_{\rm II}$-mode is decreasing with increasing rotation rate, while the frequency of the F-mode is increasing.

For both sequences A and B (which have a fixed strength of differential rotation, $\hat{A} = 1$) the $F_{\rm II}$-mode is excited at the same level as the F-mode, by the perturbation shown in Eq. (3) (the amplitude of the Fourier transform is similar for both modes). Varying the degree of differential rotation (for the same model and the same applied perturbation) we find that, while the amplitude of the F-mode remains constant, the amplitude of the $F_{\rm II}$-mode decreases as the star becomes less differentially rotating. In the limit of uniform rotation, there still exists a peak in the Fourier transform, corresponding to the $F_{\rm II}$ mode, although it has an amplitude much smaller than the main F-mode (see Figure 8, which compares the Fourier transforms for models B7 and BU7). Extracting the eigenfunction of the radial velocity perturbation, in the equatorial plane, for model BU7, shows

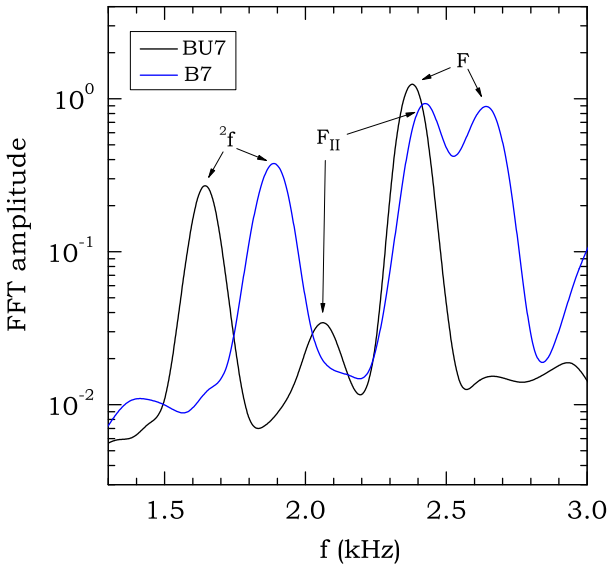

Figure 8. Comparison of integrated Fourier amplitudes of the density evolution for a differentially rotating (B7) and a uniformly rotating (BU7) model. The peaks corresponding to the fundamental quasi-radial mode F, the additional fundamental mode $F_{\rm II}$ and the fundamental $l = 2$ mode are shown.

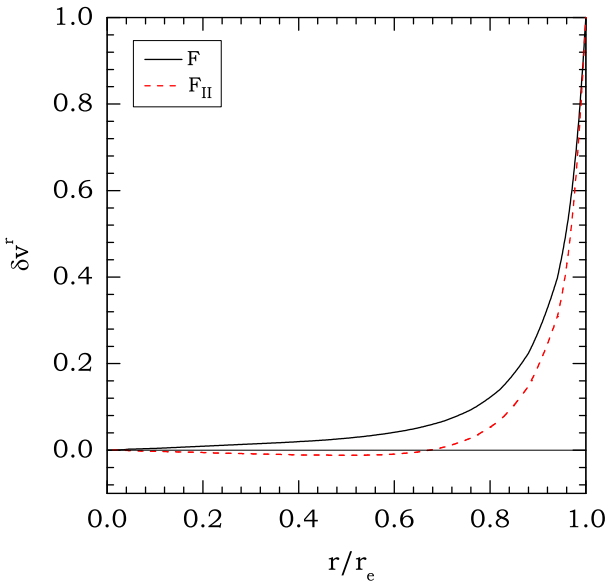

Figure 9. Comparison of the eigenfunctions, in the equatorial plane, corresponding to variations in the velocity component v^r for the fundamental quasi-radial mode F and for the additional fundamental mode $F_{\rm II}$ (for the uniformly rotating model BU7)

that the eigenfunction of the $F_{\rm II}$-mode has a node close to 70% of the equatorial radius, while the F-mode clearly has no node (see Figure 9). Even though the $F_{\rm II}$-mode has a node in the radial velocity, which is a property of a first overtone in a nonrotating star, we still refer to it as a fundamental mode, due to its degeneracy with the F-mode in a nonrotating star.

The distinction between the F-mode and the $F_{\rm II}$-mode becomes very clear in the extracted two-dimensional eigenfunctions. Figures 10 and 11 show the eigenfunction of the two modes, corresponding to the density perturbation, for the differentially rotating model B8. The eigenfunction of the F-mode is significantly modified by rotational couplings near the equatorial surface, but otherwise it is similar to the expected eigenfunction of the F-mode in a nonrotating star. In contrast, the eigenfunction of the $F_{\rm II}$ mode is similar to an F-mode eigenfunction in a nonrotating star only in the central region, but otherwise it is very different in the polar and equatorial regions. The shape of the eigenfunction in the equatorial plane (having no node in the density perturbation) is reminiscent of density perturbations in differentially rotating tori.

Is the $F_{\rm II}$-mode physical? Since our numerical code implements the Cowling approximation we cannot answer this question at present. In the Cowling approximation the energy and momentum conservation are violated. In previous simulations (Font et al. 2001) this violation of the constraints has lead to the appearance of an unphysical "fundamental" dipole mode. It is possible that the $F_{\rm II}$-mode observed in the present simulations is also an artifact of the Cowling approximation. This can only be confirmed by new simulations in full general relativity.

6 MASS-SHEDDING-INDUCED DAMPING OF PULSATIONS

Linear perturbations of rotating stars are assumed to have a vanishingly small amplitude, so that the background equilibrium star is unaffected by a linear oscillation mode. However, when one considers a finite-amplitude oscillation, then nonlinear effects can become important. Our nonlinear evolution code allows us to investigate such effects.

At low rotation rates, a small oscillation amplitude of the order of 10^{-2} does not lead to significant nonlinear effects. But, as the star approaches the mass-shedding limit, the effective gravity near the equatorial surface diminishes. Exactly at the mass-shedding limit fluid elements are only marginally bound to the surface of the star. A small radial pulsation then suffices to cause mass-shedding after each oscillation period. At an oscillation frequency around 2.3 kHz (in the Cowling approximation), matter that has been shed from the star does not have the time to fall back before more matter is shed (this statement applies to the specific example with an initial pulsation amplitude of the order of 10^{-2}, that is studied here – more generally, the fall-back time will depend on the initial amplitude). In this way, a low-density toroidal envelope is created in the equatorial region, which expands with every oscillation period.

Figure 12 shows the profile of the specific internal energy ϵ at two different times, for the uniformly rotating model BU9, which is at the mass-shedding limit. It is clearly seen that the matter is shed in the form of high-entropy shock waves. A first shock wave, shown at t=0.14ms, leaves the star as a result of the initial perturbation applied to the equilibrium model. After one oscillation period, a second shock wave leaves the star and both shock waves are shown at t=0.92ms. In the same fashion, consecutive shock waves are created after each oscillation period and the density in the toroidal envelope gradually increases.

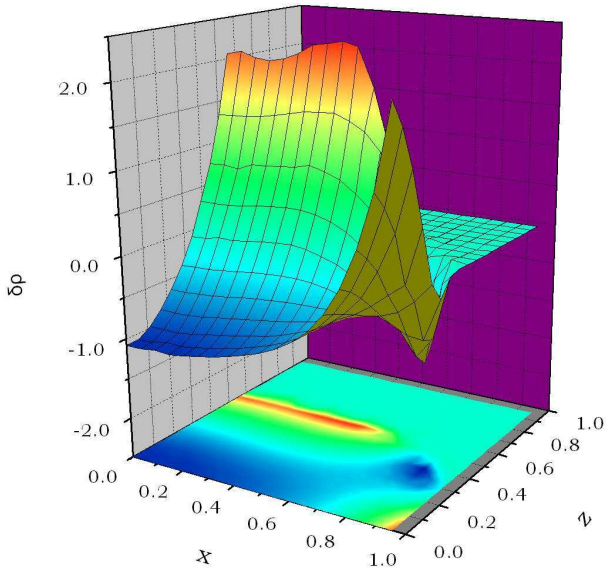

Figure 10. Two-dimensional eigenfunction of the density perturbation, corresponding to the $l = 0$ fundamental mode for the differentially rotating model B8.

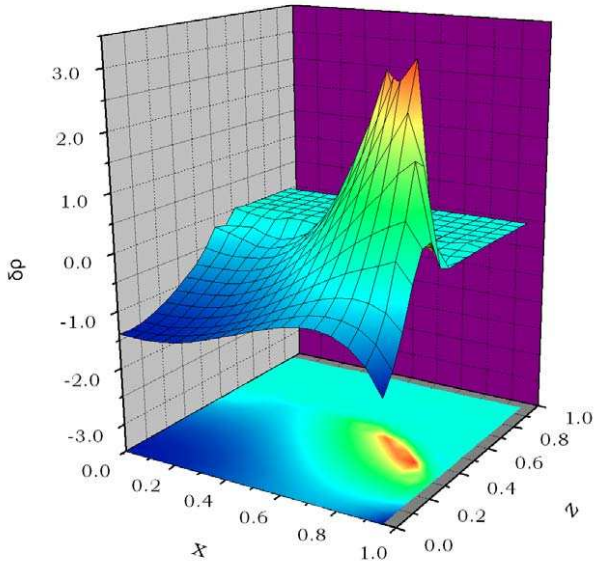

Figure 11. Same as Figure 10, but for the additional fundamental mode $F_{\rm II}$ (see discussion in Section 5).

Since matter is shed from the star in the form of shocks, they carry away kinetic energy, to the expense of the pulsational energy. In this way, the pulsations of the star are gradually damped. Figure 13 shows a comparison between the time-evolution of the central rest-mass density in the slowly rotating model BU1 and model BU9. It is evident that the damping of the pulsations due to mass-shedding is very strong. The damping will also be effective in stars which rotate at somewhat smaller rotation rates. The precise damping rate will depend on several factors, such as the amplitude of the pulsation, the rotation rate of the star, the EOS etc. The assumption of the Cowling approximation which we have adopted in our simulations will also affect the damping rate, as it causes an imbalance between the different forces acting on a fluid element on the equatorial surface of the star. Simulations which take into account the time-evolution of the gravitational field during the oscillations should yield more accurate damping rates.

Our finding of the mass-shedding induced damping of pulsations in critically rotating stars can have severe consequences for unstable pulsation modes, such as f-modes and r-modes, since, over a timescale of several seconds, even a very small damping rate could suffice to saturate their amplitude at values much less than order unity.

7 DETECTABILITY OF GRAVITATIONAL WAVES

Pulsating rotating neutron stars are gravitational-wave sources that depend on several parameters (EOS, mass, angular momentum, differential rotation law, initial amplitude, damping mechanisms etc.). All these parameters may have different effects on the oscillation spectrum of the star and, therefore, the successful extraction of the physical characteristics of the source from the gravitational-wave signal will be difficult to achieve. It is important to isolate each effect on the gravitational waveform in order to find general trends. If independent information about the source (a gravitational-wave burst, or optical, neutrino or gamma-ray signals in the case of core collapse; a gravitational-wave chirp in the case of a binary merger) can distinguish between isolated neutron star formation and binary merger, then this could be used to constrain the interesting range of several parameters. Thus, a combined filter that includes both a pre-formation characteristic signal and several damped pulsation modes will enhance the total signal to noise ratio (see Kokkotas, Apostolatos & Andersson, 2001, for extraction of the characteristic parameters of a damped monochromatic gravitational waves, through matched filtering).

In the core collapse simulations by Dimmelmeier et al. (2001, 2002a, 2002b) the quasi-periodic gravitational waves emitted during core collapse were found to have frequencies less than roughly 1.1 kHz and our computed frequencies of $l = 0$ and $l = 2$ modes agree with this, as discussed in Section 4.1. Such frequencies are still within the range of current laser-interferometric detectors. However, the above frequencies are typical only for certain EOSs. The fundamental $l = 2$ f-mode frequency of the nonrotating model of sequence A is at the lower end of the corresponding frequency range for $1.4M_{\odot}$ models, constructed with a large sample of different realistic EOSs, which range from ~ 1.35 kHz (for extremely stiff EOSs) to ~ 3.6 kHz (for extremely soft EOSs), see e.g. Andersson & Kokkotas (1998). A similar range of frequencies, for different EOSs, exists for the fundamental $l = 0$ mode, for stars of $1.4M_{\odot}$ mass. Based on the empirical relations constructed in Section 4.1, we estimate that, depending on the stiffness of the high-density EOS, the frequency range of quasi-periodic gravitational waves during core collapse could be as low as 0.65 to 1.35 kHz for extremely stiff EOSs and as high as 1.8 to 3.6 kHz for extremely soft EOSs. The higher frequency range would be accessible for gravitational-wave detection only with detec-

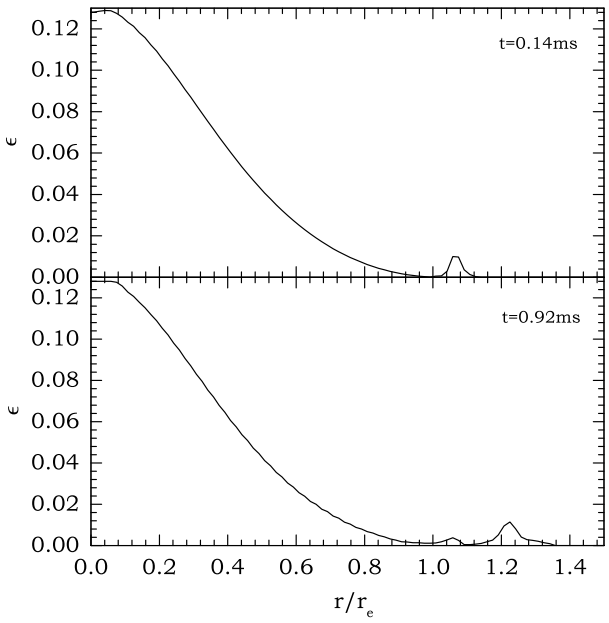

Figure 12. Profiles of the internal energy ϵ showing the propagation of shocks, generated due to radial pulsations at the surface of the star. At $t = 0.14$ms, a first shock is shown to propagate away from the star. At $t = 0.92$ms, a second shock is propagating in the rarefaction region created by the first shock. A shock is produced after each period of the fundamental quasi-radial mode F. Pulsational energy is carried away by these shocks and a high-entropy envelope forms in the equatorial region surrounding the star.

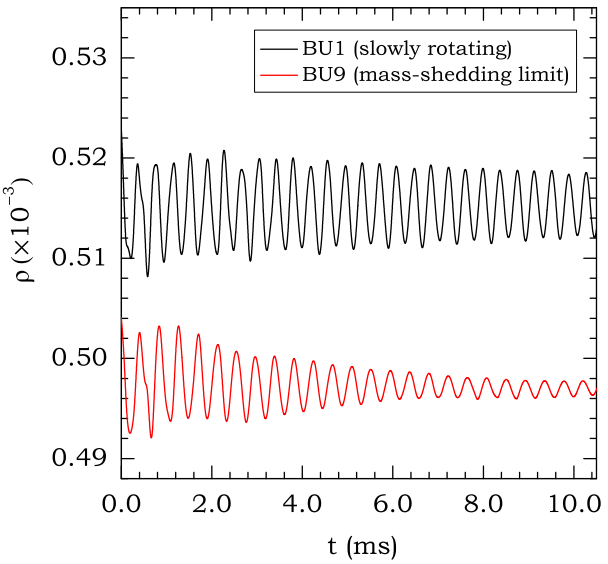

Figure 13. Damping of nonlinear pulsations for a star rotating at the mass-shedding limit. For a slowly rotating star the pulsations are not damped (except by numerical viscosity). The time-evolution of the density is shown at half-radius in the star (for a better comparison, the lower curve was displaced by a fixed amount on the vertical axis). For an initial mode amplitude of 1%, the nonlinear damping occurs on a dynamical timescale.

tors such as the proposed wide-band dual sphere (Cerdonio et al. 2001).

In the case of a neutron-star binary merger, the high-frequency quasi-periodic oscillations excited in the hypermassive neutron star could last for a large number of oscillation periods, since the damping due to a low-density envelope should be much weaker than in the core collapse case. Thus, the quasi-periodic signal could be enhanced significantly by matched filtering.

8 DISCUSSION

Using an axisymmetric general relativistic hydrodynamics code we have studied nonlinear pulsations of uniformly and differentially rotating neutron stars. We have performed time-dependent numerical simulations of a large sample of initial models which were slightly perturbed away from hydrostatic equilibrium. The time-evolutions have been analyzed using Fourier transforms at several points inside the stars, which enables the extraction of the two-dimensional eigenfunction for each mode. Our attention has been focused on two different sequences of uniformly and differentially rotating stars, for which we have obtained the pulsation frequencies for the two lowest-order quasi-radial ($l = 0$) and quadrupole ($l = 2$) modes. We have found that differentially rotating models can reach significantly lower pulsation frequencies than uniformly rotating models of the same rest-mass. In addition, our simulations show that the fundamental quasi-radial mode is split into two different sequences. This new mode has been most clearly observed in the fastest differentially rotating models. The centrifugal forces and the degree of differential rotation have significant effects on the mode-eigenfunctions. Most notably, axisymmetric nonradial modes acquire a nonzero density variation at the center of the star, due to coupling to lower-order terms in the eigenfunction. However, both the splitting of the fundamental mode and the nonzero central density variations of nonradial modes could be due to the use of the Cowling approximation.

We have found that near the mass-shedding limit the pulsations are damped due to shocks forming at the surface of the star, when matter is shed in the equatorial region during each pulsation cycle. The damping rate should depend on the amplitude of the pulsations and on the rotation rate of the star. This new damping mechanism may set a small saturation amplitude for modes that are unstable to the emission of gravitational radiation. The nonlinear development of pulsations when subject to this strong damping depends on the adopted EOS during the time-evolution. If one restricts the perfect fluid to remain isentropic, by assuming that the usual polytropic EOS holds throughout the evolution, then this restriction does not allow for real shocks to form and propagate away from the star, even though discontinuities appear in the fluid variables in this case as well (actually, such discontinuities are larger than the corresponding discontinuities in the non-isentropic case, for the same mode-amplitude, due to kinetic energy conservation). Instead of propagating shocks, one obtains a behaviour that is reminiscent of the "wave-breaking" of large-amplitude r-modes in rapidly rotating stars, in nonlinear simulations by Lind-

blom, Tohline & Valisneri (2001)[4]. In contrast, the correct approach is to use a *nonisentropic* EOS during the evolution, such as the ideal fluid EOS used in our simulations, which allows for physically realistic shocks to form and propagate. We note that in the simulations by Lindblom et al. (2001) the growth in the amplitude of the unstable r-mode was accelerated by a large factor, leading to the "wave-breaking" and the sudden destruction of the mode. We conjecture that if one would use a nonisentropic EOS and would not accelerate the natural r-mode growth time, then a balance between the growth rate due to gravitational-radiation reaction and the damping rate due to shock-dissipation caused by mass-shedding could be obtained at some amplitude less than order unity. This discussion is relevant, of course, only if in very rapidly rotating stars the mass-shedding-induced damping limits the nonlinear amplitude of unstable modes before other nonlinear saturation mechanisms can dominate. Examples of other nonlinear saturation mechanisms are saturation due to the interaction of differential rotation with a magnetic field (Rezzolla, Lamb & Shapiro, 2000; Rezzolla et al. 2001a, 2001b), hydrodynamical instabilities of large-amplitude nonlinear oscillations (Gressman et al. 2002) and nonlinear couplings to other damped modes (Schenk et al. 2002; Morsink 2002; Arras et al. 2003). At present, it is still unclear what the relation, if any, between the latter two mechanisms is (in the case of r-mode oscillations). Which nonlinear saturation mechanism sets the maximum amplitude of unstable modes could depend on the rotation rate and the magnetic field strength of the star.

ACKNOWLEDGMENTS

It is a pleasure to thank Massimo Cerdonio, Harry Dimmelmeier, Kostas Kokkotas, José Pons, Hans Ritter, Henk Spruit and Arun Thampan for helpful discussions. We also thank the referee, Prof. L. Rezzolla, for useful comments and Emanuele Berti for a careful reading of the manuscript. Financial support for this research has been provided by the EU Network Programme (Research Training Network Contract HPRN-CT-2000-00137). T.A.A. acknowledges financial support from the Special Accounts for Research Grants of the University of Athens (grant 70/4/4056). J.A.F. acknowledges financial support from the Spanish Ministerio de Ciencia y Tecnología (grant AYA 2001-3490-C02-01). The computations were performed on the NEC SX-6 at the Rechenzentrum Garching (Germany).

REFERENCES

Andersson, N., Kokkotas, K. D., 1998, MNRAS, 299, 1059
Arras, P., Flanagan, E. E., Morsink, S. M., Schenk, A. K., Teukolsky, S. A., Wasserman, I., 2003, Astrophys. J., 591, 1129
Baumgarte, T. W., Shapiro, S. L., Shibata, M., 2000, Astrophys. J., 528, L29
Carroll, B. W., Zweibel, E. G., Hansen, C. J., McDermott, P. N., Savedoff, M. P., Thomas, J. H., Van Horn, H. M., 1986, Astrophys. J., 305, 767
Cerdonio, M., Conti, L., Lobo, J. A., Ortolan, A., Taffarello, L., Zendri, J. P., 2001, Phys. Rev. Lett., 87, 031101
Cook, J. N., Shapiro, S. L., Stephens, B. C., 2003, astro-ph/0310304
Dimmelmeier, H., Font, J. A., Müller, E., 2001, Astrophys. J., 560, L163
Dimmelmeier, H., Font, J. A., Müller, E., 2002a, Astron. Astrophys., 388, 917
Dimmelmeier, H., Font, J. A., Müller, E., 2002b, Astron. Astrophys., 393, 523
Font, J. A., Living Rev. Relativity, 2003, 6, 4
Font, J. A., Stergioulas, N., Kokkotas, K. D., 2000, MNRAS, 313, 678
Font, J. A., Dimmelmeier, H., Gupta, A., Stergioulas, N., 2001, MNRAS, 325, 1463
Font, J. A., Goodale, T., Iyer, S., Miller, M., Rezzolla, L., Seidel, E., Stergioulas, N., Suen, W. M., Tobias, M., 2002, Phys. Rev. D, 65, 084024
Friedman, J. L., Lockitch, K. H., 2001, in Proc. 9th Marcel Grossman Meeting, eds. Gurzadyan, V., Jantzen, R., Ruffini, R., gr-qc/0102114
Friedman, J. L., Ipser, J. R., Parker, L., 1986, Astrophys. J., 304, 115
Fryer, C. L., Holz, D .E., Hughes, S. A., Warren, M. S., 2002, astro-ph/0211609
Gressman, P., Lin, L.-M., Suen, W.-M., Stergioulas, N., Friedman, J. L., 2002, Phys. Rev. D., 66, 041303(R)
Hartle, J. B., Friedman, J. L., Astrophys. J., 1975, 196, 653
Heger, A., Woosley, S. E., 2003, in Proc. Woods Hole, *Gamma-Ray Bursts and Afterglow Astronomy* (AIP), in press
Heger, A., Woosley, S. E., Langer, N., Spruit, H. C., 2003, in Proc. IAU Symp. 215, *Stellar Rotation*, eds. Maeder, A., Eenens, P., astro-ph/0301374
Hegyi, D. J, 1977, Astrophys. J., 217, 244
Ivanova, N., Podsiadlowski, Ph., 2003, in *From Twilight to Highlight: the Physics of Supernovae*, eds. Hilledrandt, W., Leibundgut, B. (Springer, Berlin) p. 19
Jones, P .B., 2001, Phys. Rev. Lett., 86, 1384
Kokkotas, K. D., Andersson, N., 2001, in Proc. SIGRAV XIV, Genoa 2000, Springer-Verlag, gr-qc/0109054
Kokkotas, K. D., Apostolatos, T. A., Andersson, N., 2001 MNRAS, 320, 307
Kokkotas, K. D., Schmidt, B., 1999, Living Rev. Relativity, 2, 2
Komatsu, H., Eriguchi, Y., Hachisu, I., 1989a, MNRAS, 237, 355
Komatsu, H., Eriguchi, Y., Hachisu, I., 1989b, MNRAS, 239, 153
Kotake, K., Yamada, S., Sato, K., 2003, Phys. Rev. D, 68, 044023
Langer, N., Yoon, S.-C., Petrovic, J., Heger, A., 2003, astro-ph/0302232
Lai, D., Shapiro, S. L., 1995, Astrophys. J., 442, 259
Lindblom, L., Owen, B. J., 2002, Phys. Rev. D, 65, 063006
Lindblom, L., Tohline, J. E., Vallisneri, M., 2001, Phys. Rev. Lett., 86, 1152
Liu, Y. T., Lindblom, L., 2000, MNRAS, 324, 1063
Liu, Y. T., Shapiro, S. L., 2003, gr-qc/0312038
McDermott, P. N., Savedoff, M. P., Van Horn, H. M., Zweibel, E. G., Hansen, C. J., 1984, Astrophys. J., 281, 746
Middleditch, J., 2003, astro-ph/0311484
Morsink, S. M., 2002, Astrophysical J., 571, 435
Morsink, S. M., Stergioulas, N., Blattnig, S. R., 1999 Astrophys. J., 510, 854
Mönchmeyer, R., Schäfer, G., Müller, E., Kates, R. E., 1991, Astron. Astrophys., 246, 417
New, K., 2003, Living Rev. Relativity, 6, 2
Nice, D. J., Splaver, E. M., Stairs, I. H., 2003, astro-ph/0311296
Nozawa, T., Stergioulas, N., Gourgoulhon, E., Eriguchi, Y., 1998, Astron. Astrophys. Suppl., 132, 431
Ott, C. D, Burrows, A., Livne, E, Walder, R., 2003, astro-ph/0307472

[4] We note that, in rapidly rotating stars, the r-mode velocity field has a significant radial component.

Podsiadlowski, Ph., Langer, N., Poelarends, A. J. T., Rappaport, S., Heger, A., Pfalh, E, 2003, astro-ph/0309588
Pons, J. A., 2003, personal communication
Pfahl, E., Rappaport, S., Podsiadlowski, Ph., Spruit, H., 2002, Astrophys. J., 574, 364
Rezzolla, L., Lamb, F.K., Shapiro, S.L., 2000 Astrophys. J., 531, L139
Rezzolla, L., Lamb, F.K., Marković, D., Shapiro, S.L., 2001a Phys. Rev. D, 64, 104013
Rezzolla, L., Lamb, F.K., Marković, D., Shapiro, S.L., 2001b Phys. Rev. D, 64, 104014
Schenk, A. K., Arra, P., Flanagan, É. É., Teukolsky, S. A., Wasserman, I., 2002, Phys. Rev. D., 65, 024001
Shapiro, S. L., 2000, Astrophys. J., 544, 397
Shibata, M., 2003, Phys. Rev. D, 67, 024033
Shibata, M., Taniguchi, K., Uryū, K., 2003, Phys. Rev. D, 68, 084020
Shibata, M., Uryū, K., 2000, Phys. Rev. D, 61, 064001
Shibata, M., Uryū, K., 2002, Prog. Theor. Phys., 107, 265
Sperhake, U., 2002, PhD Thesis, gr-qc/0201086
Sperhake, U., Papadopoulos, P., Andersson, N., 2001, gr-qc/0110487
Spruit, H. C., 2002, Astron. Astrophys., 381, 923
Stergioulas, N., 2003, Living Rev. Relativity, 6, 3
Stergioulas, N., Friedman, J. L., Astrophys. J., 1995, 444, 306
Stergioulas, N., Friedman, J. L., Astrophys. J., 1998, 492, 301
Stergioulas, N., Font, J. A., 2001, Phys. Rev. Lett., 86, 1148
van Dalen, E. N. E., Dieperink, A. E. L., 2003, nucl-th/0311103
Villain, L., Pons, J. A., Cerdá-Durán, P., Gourgoulhon, E., 2003, astro-ph/0310875
Watts, A. L., Andersson, N., 2002, MNRAS, 333, 943
Yoshida, S., Eriguchi, Y., 1999, Astrophys. J., 515, 414
Yoshida, S., Eriguchi, Y., 2001, MNRAS, 322, 389
Yoshida, S., Kojima, Y., 1997, MNRAS, 289, 117
Yoshida, S., Rezzolla, L., Karino, S., Eriguchi, Y., 2002 Astrophys. J., 568, L41
Yuan, Y., Heyl, J. S., 2003, astro-ph/0305083
Zwerger, T., Müller, E., 1997, 320, 209